Journal of Mathematical Biology (2019) 78:1089–1113
https://doi.org/10.1007/s00285-018-1303-1

Mathematical Biology

Optimal time-profiles of public health intervention to shape voluntary vaccination for childhood diseases

Bruno Buonomo[1] · Piero Manfredi[2] · Alberto d'Onofrio[3]

Received: 18 September 2017 / Revised: 10 September 2018 / Published online: 2 November 2018
© Springer-Verlag GmbH Germany, part of Springer Nature 2018

Abstract

In order to seek the optimal time-profiles of public health systems (PHS) Intervention to favor vaccine propensity, we apply optimal control (OC) to a SIR model with voluntary vaccination and PHS intervention. We focus on short-term horizons, and on both continuous control strategies resulting from the forward–backward sweep deterministic algorithm, and piecewise-constant strategies (which are closer to the PHS way of working) investigated by the simulated annealing (SA) stochastic algorithm. For childhood diseases, where disease costs are much larger than vaccination costs, the OC solution sets at its maximum for most of the policy horizon, meaning that the PHS cannot further improve perceptions about the net benefit of immunization. Thus, the subsequent dynamics of vaccine uptake stems entirely from the declining perceived risk of infection (due to declining prevalence) which is communicated by direct contacts among parents, and unavoidably yields a future decline in vaccine uptake. We find that for relatively low communication costs, the piecewise control is close to the continuous control. For large communication costs the SA algorithm converges towards a non-monotone OC that can have oscillations.

Keywords Vaccination · Human behavior · Public health system · Communication · Optimal control · Simulated annealing · Forward–backward sweep method

Mathematics Subject Classification 92D30 · 49J15 · 49N90 · 91A80 · 91A22

✉ Alberto d'Onofrio
alberto.donofrio@i-pri.org

Bruno Buonomo
buonomo@unina.it

Piero Manfredi
manfredi@ec.unipi.it

[1] Department of Mathematics and Applications, University of Naples Federico II, via Cintia, 80126 Naples, Italy

[2] Department of Economics and Management, University of Pisa, Via Ridolfi 1, 56124 Pisa, Italy

[3] International Prevention Research Institute, 95 cours Lafayette, 69006 Lyon, France

1 Introduction

In the last ten years, a new research field in epidemiology has emerged: the *behavioral epidemiology* (BE) of infectious diseases (Manfredi and d'Onofrio 2013; Funk et al. 2010). BE focuses on the feedbacks of human behavior on the transmission and control of infections (Manfredi and d'Onofrio 2013; Funk et al. 2010). In traditional models (Anderson et al. 1992; Capasso 1993), individuals are modeled as passive particles randomly interacting according to the mass-action principle (Manfredi and d'Onofrio 2013; Wang et al. 2016). This assumption inadequately represents contemporary scenarios, where individuals-based on information and rumors on the spread of diseases–modify their social behavior and their propensity to vaccinate (Manfredi and d'Onofrio 2013; d'Onofrio et al. 2007; Wang et al. 2016). The study of the impact of human decisions on the vaccine uptake under voluntary vaccination is a major area of BE research (Manfredi and d'Onofrio 2013; Wang et al. 2016; Bauch 2005)

Indeed, if vaccination is no longer mandatory, then the high degrees of disease control allowed by vaccine-induced herd immunity achieved in the past, jointly with the high standard of health of western societies (Manfredi and d'Onofrio 2013; d'Onofrio et al. 2011), can favor the spread of *information-dependent* behavior (Manfredi and d'Onofrio 2013; Buonomo et al. 2013). On the one hand, in periods of low prevalence families might tend to overweight information and rumors on vaccine side-effects and their propensity to vaccinate might decline. On the other hand, periods of high infection prevalence or of outbreaks can enhance the propensity to vaccinate.

BE research has shown that this behavior makes disease elimination unfeasible even when temporarily coverages is near 100% in epochs of high perceived risk, and triggers large recurrent epidemics (Bauch 2005; Manfredi and d'Onofrio 2013; d'Onofrio et al. 2007, 2011).

In Oraby et al. (2014) it is stressed that some BE models identify vaccine refusal as the *typical* behavior, whereas it should be [as in d'Onofrio et al. (2007)] the atypical one, as shown by the large vaccine coverages that can be observed worldwide.

In d'Onofrio et al. (2012) a simple explanation of vaccine acceptance as the typical behavior was proposed: even if vaccination is voluntary the public health system (PHS) can favor vaccine propensity by providing influential information on infection and vaccines. It is the 'persuasion success' of PHS efforts that makes vaccine acceptance the typical behavior. Indeed, the model suggests that infection could be eliminated for adequate levels of effort.

A shortcoming of d'Onofrio et al. (2012) is that the communication effort by the PHS is modeled as constant. In the practice, such effort is not constant, due to a range of epidemiological and economical variables, including the disease burden and the economic and human costs of immunization.

For such a model the determination of a suitable PHS effort that minimizes economic costs under given constraints in a given time-horizon calls for the application of Optimal Control (OC) theory, which is our aim.

Applications of OC theory (Schättler and Ledzewicz 2012) to classical mathematical epidemiology date back to the seventies (Hethcote and Waltman 1973; Morton and Wickwire 1974; Sethi and Staats 1978; Wickwire 1977). Recently, simple deterministic numerical schemes have been introduced (Aniţa et al. 2011; Lenhart and

Workman 2007) that renewed interest in application of OC to classical mathematical epidemiology (Asano et al. 2008; Buonomo 2011; Betta et al. 2016; Blayneh et al. 2010; Bolzoni et al. 2014; Demasse et al. 2016; Hansen and Day 2011; Jung et al. 2009, 2002; Laguzet and Turinici 2015a; Lee and Castillo-Chavez 2015; Onyango and Müller 2014; Rachah and Torres 2016; Rowthorn and Walther 2017) and to BE (Kassa and Ouhinou 2015; Laguzet and Turinici 2015b; Doutor et al. 2016).

Among the above mentioned deterministic algorithms, we may cite the Forward–Backward sweep (FBS) algorithm (Hackbusch 1978) and the gradient methods (Aniţa et al. 2011). These algorithms are approximation methods built on the necessary conditions obtained by the maximum principle that the control and the state variables need to satisfy (Pontryagin et al. 1962). In particular, the FBS, which will be used here, provides a numerical approximation to the differential-algebraic system consisting of the state and co-state differential equations and the optimality condition (derived from maximization of the Hamiltonian) which in many problems may be expressed by an algebraic equation.

There is an interesting issue related to the use of optimal solutions in applied problems, which is very important for the study of the PHS effort to favor vaccine uptake. Indeed, in OC theory the control function (generally denoted by $u(t)$) is usually assumed to be a generic Lebesgue integrable function (LIF). Although this assumption is adequate in many domains, it becomes unrealistic when $u(t)$ is the outcome of a range of human interventions, as for vaccination programmes. The complex machinery of PHS has slow reactions, making impossible to update the strategy on a weekly or even monthly base. In such scenarios, control functions should instead be represented as a well-defined subset of LIFs: piece-wise constant functions (Betta et al. 2016; Faber et al. 2005). Moreover, the intervals where the control $u(t)$ is constant must be quite long, i.e. $u(t)$ spans in a finite-dimensional space with low dimension (typically the number of changes of strategy per year times the number of years of the chosen time horizon). This is at variance both with theoretical OC solutions, which are infinite dimensional, and with their numerical approximations, which have large dimensions. Indeed, the numerical approximation of OC requires short timesteps, which are smaller than few days, sometime few hours. This results on the whole time-horizon in a dimension that is finite but is very large.

In this circumstance the original OC problem is transformed into a new problem: finding the global minimum of a real function of a finite number of parameters by using heuristic optimization algorithms, which can be deterministic or stochastic (Banga and Seider 1996; Schoen 1991). Among the latter class, one of the most widely adopted is the *Simulated annealing* (SA) (Kirkpatrick et al. 1983; Faber et al. 2005; Henderson et al. 2003; Martínez-Alfaro 2010; Salamon et al. 2002).

Based on these considerations, in this work we employ the OC theory and SA-based heuristic optimization to assess how epidemiological and economic factors affect the communication effort of the PHS. Namely, this is done by seeking a time-variable control in the model introduced in d'Onofrio et al. (2012) such that the costs for the PHS during a given time period are minimized. In particular, our OC problem seeks to minimize total costs due to both the disease burden, vaccination costs (including costs from adverse events) and communication costs.

As in Bauch (2005), we consider vaccines targeted at childhood infectious diseases such as measles, mumps and pertussis. In particular, we will focus on short term horizons and investigate the ability of the PHS to effectively increase vaccine uptake in a short time span, departing from an initial situation where vaccine uptake was unsatisfactorily low. This situation was well represented by the case of measles in Italy before the large efforts to expand vaccination carried out in the last decade (d'Onofrio et al. 2012).

This approach will also allow us to show, with a specific example, how two different numerical approaches (the FSB deterministic algorithm and the SA stochastic algorithm) to OC can usefully be employed.

The paper is organized as follows. In Sect. 2 the model introduced in d'Onofrio et al. (2012) is reviewed. In Sect. 3 the OC problem is formulated and parametrized. In Sect. 4 we determine OC candidate functions by using the FBS algorithm. In Sect. 5 we validate the nature of global minimum of the candidate OC by employing the SA stochastic algorithm. Concluding remarks follow in Sect. 6.

2 The basic model and PHS intervention

In this section we shortly review models and main results of d'Onofrio et al. (2011, 2012), Wang et al. (2016), Buonomo et al. (2018). In d'Onofrio et al. (2011) the following information-dependent SIR model without disease-related fatalities and with non mandatory vaccination at birth was considered:

$$\begin{aligned} \dot{S} &= \mu(1-p) - \mu S - \beta SI \\ \dot{I} &= \beta SI - (\mu+\nu)I \\ \dot{p} &= kp(1-p)\left(\theta_1 I - p\right), \end{aligned} \tag{1}$$

where the state variables S, I, p represent the fraction of susceptible individuals in the population (S), the fraction of infectious individuals (I), and the proportion of parents of newborns who is favorable to vaccination (p), taken as a proxy of vaccine uptake af time t. The dynamics of the vaccinated fraction, denoted as V, is linearly depending on $p(t)$ and it reads as follows: $\dot{V} = \mu p - \mu V$. Finally, the dynamics of the removed fraction (represented by the state variable R) trivially follows: $R = 1 - S - I - V$. Since the dynamics of the pair (V, R) elementarily derives from the dynamics of the triple (S, I, p), in the following we will only focus on the latter three state variables, as in d'Onofrio et al. (2011, 2012). The parameters are positive constants: μ is the death rate, assumed to be identical to the birth rate; ν is the recovery rate; β is the contact rate.

Note that the dynamics of p is governed by an imitation model (Hofbauer and Sigmund 1998). This extends the equation for adoption by *imitation* (Mahajan and Peterson 1985) by including agents' payoffs. The net payoff gain of immunization (ΔQ) which is perceived from person-to-person contacts has the following general *information-dependent* form introduced in d'Onofrio et al. (2011): $\Delta Q = \theta I - \eta p$, where θI, ($\theta > 0$) defines the perceived risk associated to the disease (taken as prevalence-dependent), while ηp ($\eta > 0$) defines the perceived risk of suffering

vaccine adverse events (VAE). This risk is taken to be a linear function of actual vaccine uptake p. The third equation in 1 then follows by setting $\theta_1 = \theta/\eta$, which represents a normalized measure of the relative risk of infection compared to the risk of VAE. In this context, k is the (normalized) index of imitation or *internal* influence. We stress that the imitation game approach in d'Onofrio et al. (2011), which was based on the classical economy-oriented interpretation of evolutionary game theory, has been given a semi-mechanistic interpretation in Wang et al. (2016) as the result of a mutual *contagion of ideas* between the group of parents that are favorable to vaccinate their children (whose fraction at time t is given by $p(t)$) and the group that is not favorable to vaccination (whose fraction at time t is given by: $a(t) = 1 - p(t)$).

Model (1) admits a 'behavior–induced' endemic equilibrium

$$E = (S_e, \quad I_e(\theta), \quad p_e) \equiv \left(\frac{1}{R_0}, \quad \frac{1 - S_e}{1 + \frac{\nu}{\mu} + \theta}, \quad \theta I_e(\theta) \right), \tag{2}$$

where $R_0 = \beta/(\mu + \nu)$ is the basic reproduction number of SIR model.

Although the equilibrium E is independent of k, its stability does. Namely, for sufficiently large values of θ one may find intervals $[k_1(\theta), k_2(\theta)]$ where the infection prevalence shows sustained oscillations, whereas outside of these intervals E is locally asymptotically stable.

Model (1) was extended in d'Onofrio et al. (2012) to include the effects of the communication actions by the PHS aimed at increasing vaccine uptake, by assuming that the effort of the PHS per time unit is proportional to the fraction of parents unfavorable to vaccination. The resulting equation for p is:

$$\dot{p} = k(1 - p)\,(\theta_1 I - p)\,p + G(t)(1 - p). \tag{3}$$

In view of the mechanistic interpretation given in Wang et al. (2016), the term $G(t)(1 - p)$ is nothing else than the influx of parents that switched their vaccine propensity thanks to the action of the PHS. It is useful to normalize the function G:

$$\gamma(t) = \frac{G(t)}{k\theta_1},$$

yieding:

$$\dot{p} = k\theta_1(1 - p)\left[(I - \alpha p)\,p + \gamma(t)\right], \tag{4}$$

where $\alpha = 1/\theta_1$ is a measure of the (relative) perceived risk of VAE (i.e., of the propensity to vaccine refusal). The model then reads

$$\begin{aligned} \dot{S} &= \mu(1 - p) - \mu S - \beta SI \\ \dot{I} &= \beta SI - (\mu + \nu)I \\ \dot{p} &= k\theta_1(1 - p)\left[(I - \alpha p)\,p + \gamma(t)\right]. \end{aligned} \tag{5}$$

Note that in d'Onofrio et al. (2012) only the case of constant $\gamma(t)$ was actually considered: $\gamma(t) = x$. In particular, if $x \geq \alpha p_c^2$, where $p_c = 1 - 1/R_0$ is the critical

immunization threshold (Anderson et al. 1992), then it can be seen that (d'Onofrio et al. 2012)

$$p(t) \to min(1, (x/\alpha)^{0.5}), \qquad I(t) \to 0. \tag{6}$$

In other words, there exists a threshold equal to αp_c^2 for x such that if this threshold is exceeded, i.e. if $x \geq \alpha p_c^2$, then $p(t)$ tends to an equilibrium value p_e greater than the elimination threshold p_c, while the prevalence $I(t)$ tends to zero, so that the infection is eliminated.

On the contrary, if $x < \alpha p_c^2$, then there is an endemic equilibrium (S_e, I_e, p_e) such that (d'Onofrio et al. 2012):

$$\begin{aligned} S_e &= 1/R_0, \\ I_e(p_e) &= \frac{\mu}{\mu+\nu}(p_c - p_e), \end{aligned} \tag{7}$$

and p_e is given by the unique positive solution of the following equation:

$$p_e\,(I_e(p_e) - \alpha p_e) + x = 0. \tag{8}$$

That is,

$$p_e(x) = \frac{\frac{\mu p_c}{\mu+\nu} + \sqrt{\frac{\mu^2 p_c^2}{(\mu+\nu)^2} + 4x\left(\alpha + \frac{\mu}{\mu+\nu}\right)}}{2\left(\alpha + \frac{\mu}{\mu+\nu}\right)}. \tag{9}$$

3 The OC problem and parametrization

3.1 The OC problem

We now consider the case in which the PHS attempts to optimally tune its temporal effort in providing information about the infection and vaccines, as represented by the function $\gamma(t)$. The aim is to minimize the total cost due to the disease and to the intervention during the time interval $[0, T]$, where T is the finite time horizon. We assume that the public effort is a Lebesgue measurable function such that:

$$0 \leq \gamma(t) \leq \gamma_{max}, \quad \text{for } t \in [0, T]. \tag{10}$$

The upper bound for γ reflects the idea that there are practical limitations on the maximum rate at which information may be spread by the PHS. The cost functional to be minimized includes the following components:

(i) *Enactment cost of the strategy*. We take:

$$J_\gamma = C_\gamma \int_0^T \gamma^2(t)dt, \tag{11}$$

where C_γ is a positive constant weight.

The quadratic cost of the control is the simplest and most widely used nonlinear representation of intervention costs in epidemiology (see e.g. Blayneh et al. 2010; Chamchod et al. 2014; Choi and Jung 2014; Lee et al. 2011, 2012; Lee and Castillo-Chavez 2015; Neilan et al. 2010; Prosper et al. 2011; Rachah and Torres 2016; Rodrigues et al. 2014; Zhao et al. 2016). This assumption underlies the idea that costs might increase non-linearly at high intervention levels. Usually the quadratic cost is adopted as *black box* assumption, but in our case it can be somehow justified. Indeed, the per time unit of the PHS effort (denoted by $j_\gamma(t)$ and whose integral is J_γ) can be written as follows:

$$j_\gamma(t) = N\mu\gamma(t)a(t)A(\gamma(t), a(t)) \tag{12}$$

where N denotes the total population, $a(t) = 1 - p(t)$ denotes, as mentioned in Sect. 2, the fraction of population adopting the 'no-vaccine' strategy, $N\mu\gamma(t)a(t)$ is the number of parents changing strategy per time unit, and $A(\gamma, a)$ is the per-capita cost for the PHS to realize strategy switching. This function is such that:

1. $\partial_\gamma A(\gamma, a) > 0$, since γ is a measure of the specific speed of strategy-change induced by the actions of the PHS. Thus the larger is this speed, the larger are the costs;
2. $\partial_a A(\gamma, a) < 0$, since the smaller (resp. larger) is the proportion of anti-vaccinators the larger (resp. smaller) is the effort needed to convince them to switch strategy. This can be qualitatively justified based on the 'continuous' flowing from vaccine hesitancy to vaccine refusal (Larson et al. 2014; Sadaf et al. 2013). Qualitatively: if a is close to 1 then it is likely that the subjects not-vaccinating their babies are hesitant more than contrary to vaccination; if after intensive action of the NHS a is close to 0, this suggests that these residual non-vaccinating parents are very likely strongly opponents to vaccination;
3. $\lim_{a\to 0^+} A(\gamma, a) = +\infty$, since when the non-vaccinating parents are very few the effort of the PHS becomes huge and the task unfeasible. This mirrors the historical evidence on smallpox for which it was impossible to eliminate all anti-vaccination groups despite its large mortality rate and also despite the large efforts world-wide to favor smallpox vaccination (Williamson 2007).

Under the above assumptions, the simplest formulation of function A is:

$$A(\gamma, a) = \frac{C_\gamma}{N\mu}\frac{\gamma}{a},$$

thus yielding the quadratic cost (12). In this way, the unitary cost tends to considerably grow as a is very small, but not so much to have $lim_{a\to 0^+}(aA) = +\infty$. Indeed, in such a case the enactment cost of the strategy may become unbounded. For example, if $A(\gamma, a) \propto \gamma/a^2$, then $j_\gamma \propto \gamma^2/(1-p)$. Therefore, the presence of such kind of j_γ in the objective functional would preclude the possibility to induce very high levels of vaccinations, which are instead observed in the epidemiological practice.

(ii) *Direct cost of vaccination*. We take:

$$J_v = K_v \int_0^T N\mu p(t)dt, \tag{13}$$

where K_v is the average direct cost of vaccine administration per person (including costs of VAE occurring during immunization).

(iii) *Disease related costs*. Assuming an average cost K_{in} for each new infection, since the number of persons that are infected per time unit is $N\beta S(t)I(t)$, it follows that:

$$J_{in} = K_{in} \int_0^T N\beta S(t)I(t)dt. \tag{14}$$

Note that $I(T)$ does not directly appear in J_{in}, which could seem suprisingly. However, since $\beta S(t)I(t) = \dot{I} + (\mu + \nu)I$, it follows that the above cost can be rewritten as follows:

$$J_{in} = K_{in}N \left(I(T) - I(0) + (\mu + \nu) \int_0^T I(t)dt \right).$$

By setting $C_v = K_v N\mu$, $C_\varphi = K_{in}N\beta$, the OC problem may be formalized as follows: find the optimal control $\gamma^*(t)$, defined in the set of admissible controls

$$\Omega = \{\gamma \mid \gamma(t) \text{ is Lebesgue measurable on } [0, T],\ 0 \le \gamma(t) \le \gamma_{max}\},$$

such that

$$J(\gamma^*) = \min_{\Omega} J(\gamma),$$

where

$$J(\gamma) = \int_0^T \left[C_\varphi S(t)I(t) + C_v p(t) + C_\gamma \gamma^2(t) \right] dt, \tag{15}$$

subject to (5) and initial data

$$S(0) = S_0 \ge 0, \quad I(0) = I_0 > 0, \quad p(0) = p_0 \ge 0, \tag{16}$$

with $S(0) + I(0) \le 1$.

We use the Pontryagin's maximum principle (Pontryagin et al. 1962) and minimize the Hamiltonian given by:

$$H(S, I, p, \gamma, \lambda_1, \lambda_2, \lambda_3, t) = C_\varphi S(t)I(t) + C_v p(t) + C_\gamma \gamma^2(t) + \sum_{i=1}^{3} \lambda_i f_i, \tag{17}$$

where $f_i, i = 1, 2, 3$, represent the right-hand sides of system (5) and $\lambda_i, i = 1, 2, 3$, are the adjoint variables. The adjoint equations are given by:

$$\dot{\lambda}_1 = -\frac{\partial H}{\partial S}; \qquad \dot{\lambda}_2 = -\frac{\partial H}{\partial I}; \qquad \dot{\lambda}_3 = -\frac{\partial H}{\partial p}. \tag{18}$$

Note that the third equation of (5) can be written as follows:

$$\dot{p} = k\theta_1 \left[\alpha p^3 - \alpha p^2 - Ip^2 + Ip + \gamma - p\gamma\right],$$

implying

$$\begin{aligned} \dot{\lambda}_1 &= -C_\varphi I + \mu\lambda_1 + \beta I\lambda_1 - \beta I\lambda_2 \\ \dot{\lambda}_2 &= -C_\varphi S + \beta S\lambda_1 - \beta S\lambda_2 + (\mu + \nu)\lambda_2 - k\theta_1(1-p)p\lambda_3 \\ \dot{\lambda}_3 &= -C_v + \mu\lambda_1 - k\theta_1\lambda_3\left[I - 2\alpha p - 2Ip + 3\alpha p^2 - \gamma\right]. \end{aligned} \tag{19}$$

The transversality equations are:

$$\lambda_i(T) = 0, \quad i = 1, 2, 3. \tag{20}$$

The existence of the OC solution $\gamma^*(t)$, is guaranteed because the requirements of classical existence theorems [i.e. Theorem III 4.1 and Corollary 4.1 in Fleming and Rishel (2012)] are satisfied. In particular, it can be easily checked that the integrand of the objective functional is convex with respect to γ and the state system can be written as a linear function of the control with coefficients dependent on time and the state variables. This ensures the existence of an optimal solution (e.g. Gaff and Schaefer 2009).

We remark that a uniqueness result may be established, for sufficiently small time-intervals, by using the approach given in Fister et al. (1998) and Joshi (2002) and also employed in Panetta and Fister (2000, 2003), Gaff and Schaefer (2009) for OC problems of epidemics and cancer treatment.

Denote by (S^*, I^*, p^*) the state corresponding to the optimal control γ^*. On the interior of the control set Ω, minimizing the Hamiltonian gives:

$$\frac{\partial H}{\partial \gamma} = 0,$$

at γ^*. That is:

$$\gamma^*(t) = \frac{k\theta_1 (p^* - 1)\lambda_3}{2C_\gamma},$$

and, taking into account the bounds on γ^*, the characterization of the OC is:

$$\gamma^* = \begin{cases} 0 & \text{if } k\theta_1 (p^* - 1)\lambda_3 < 0 \\ k\theta_1 (p^* - 1)\lambda_3/2C_\gamma & \text{if } 0 \le k\theta_1 (p^* - 1)\lambda_3 \le 2C_\gamma\gamma_{max} \\ \gamma_{max} & \text{if } k\theta_1 (p^* - 1)\lambda_3 > 2C_\gamma\gamma_{max}. \end{cases} \tag{21}$$

Table 1 Description of parameters and initial data for the OC problem

Symbol	Description	Baseline value or range
N	Total population size	6×10^7
μ	Natural birth/death rate	5.4757×10^{-5} day^{-1}
ν	Recovery rate	$1/10$ day^{-1}
R_0	Basic reproduction number	10
β	Contact rate	$R_0(\mu+\nu)$
ε	Emigration/immigration flux	2.86×10^{-8} day $^{-1}$
k	Imitation coefficient	1/90 day $^{-1}$–0.9 day $^{-1}$
θ_1	Relative risk of infection $\theta(M)$	250–4000
α	Relative risk of vaccination $\alpha(p)$	$1/\theta_1$
K_{inf}	Average cost per infection case	307 USD
K_v	Average costs per unit immunization	21.08 USD
C_φ	Total costs of infection	$K_{inf}\beta N$
C_v	Total cost of vaccinated	$K_v N\mu$
C_γ	Parameter tuning intervention cost	See text
$\gamma_{\max}$	Maximum control	$(0.5-0.7)\alpha p_c^2$
$S(0)$	Initial value for S	1/10
$I(0)$	Initial value for I	$I_e(\theta_1)$
$p(0)$	Initial value for p	$p_e(\theta_1)$

which, in short form, may be written as follows:

$$\gamma^*(t) = \min\left(\max\left(0, k\theta_1\left(p^* - 1\right)\lambda_3/2C_\gamma\right), \gamma_{max}\right).$$

3.2 Parametrization

The description of the parameters and their baseline values (or range) used in the numerical simulations are reported in Table 1. The demographic and epidemiological parameters (i. e. μ, β, ν, R_0, N) are taken from d'Onofrio et al. (2011) and Bauch (2005)). Following (Bauch 2005), a small immigration/emigration constant flux ε is also included to take into the account of immigration of infected individuals, with a positive influx $+\varepsilon$ in the second equation of (5, compensated by a negative one, $-\varepsilon$, in the first equation of (5). The model (5) reads:

$$\begin{aligned} \dot{S} &= \mu(1-p) - \mu S - \beta SI - \epsilon \\ \dot{I} &= \beta SI + \epsilon - (\mu+\nu)I \\ \dot{p} &= k\theta_1(1-p)\left[(I-\alpha p)\, p + \gamma(t)\right]. \end{aligned} \tag{22}$$

The introduction of this constant term, obviously, does not modify the optimality conditions found in Sect. 3.1.Our aim is to investigate the ability of the PHS to increase

the vaccination coverage in the short-medium term [as for measles in Italy (d'Onofrio et al. 2012)]. Moreover, medium-short horizons were adopted in the OC-based investigations of other kinds of PH interventions concerning infectious diseases (Choi and Jung 2014; Rodrigues et al. 2014). Thus, the length of the PHS planning horizon has been set to $T = 10yr$. In order to emphasize the factors underlying the difficulties to eliminate the infection, we set γ_{max} at levels below the threshold αp_c^2 that would ensure elimination in model (5) with constant γ. In particular in our simulations we will use either $\gamma_{\max} = 0.5\alpha p_c^2$ or $\gamma_{\max} = 0.7\alpha p_c^2$.

Remark 3.1 Note that the threshold αp_c^2 assumes 'small values' (d'Onofrio et al. 2012), i.e. $\gamma(t)$ takes values in a 'small' range. However, the impact of this control variable is large. For example, we remind that, in the unconstrained case, if $\gamma(t)$ even slightly exceeds the 'small' threshold αp_c^2 then it can induce the disease elimination from the target population.

Moreover, we assume that *(i)* for $t \leq 0$ no action has been enacted by the PHS; *(ii)* at $t = 0$ the system is (unless otherwise specified) at its behavior-induced endemic equilibrium forced by private information only, i.e. equilibrium (2):

$$(S(0), I(0), p(0)) = E = (S_e, I_e(\theta_1), p_e(\theta_1)).$$

Finally, to remove the complications related with the long waves predicted by the state system in its oscillatory regimes, we only select values of the behavioral parameters k, θ_1 such that equilibrium E given in (2) is locally stable. In particular, we consider the following cases that should capture all the relevant situations:

C1 $(k, \theta_1) = (1/10, 2000)$, corresponding to relatively slow imitation coefficient and large perceived relative risk of infection;
C2 $(k, \theta_1) = (1/90, 450)$, corresponding to very slow imitation and an intermediate perceived relative risk of infection;
C3 $(k, \theta_1) = (9/10, 4000)$, corresponding to relatively fast imitation and a very large perceived relative risk of infection;

As for costs parameters, the value of K_{in} is set to the best estimate of the average cost per measles case estimated for the UK following the societal perspective (Carabin et al. 2002), given by 307 USD. The unit cost of vaccination, K_v, is computed as follows: $K_v = K_{vaccine\,dose} + K_{side\,effects}$, where: $K_{vaccine\,dose}$ is the cost to deliver a single vaccine dose, which is set to the cost of a unit MMR dose, given by 19 USD, while $K_{side\,effects}$ is the average direct cost of an episode of adverse event following immunization, which is set to 2.08 USD (Carabin et al. 2002).

As for C_γ, given the lack of field data, we prefer to roughly infer its order of magnitude by the following heuristic reasoning. Let us consider the case of a constant control $\gamma = x(const.)$, where $x \in (0, \alpha p_c^2)$. In this case, the total cost per unit time at the endemic state E is given by:

$$\bar{J}(x) = K_v N \mu p_e(x) + K_{in} N \beta S_e I_e(p_e(x)) + C_\gamma x^2.$$

To figure out the order of magnitude of C_γ, we may assume that given a suitable value of x, the cost to enact the PHS information program is a fraction $\psi \in (0, 1]$,

having the same order of magnitude of the total costs arising from infection and vaccination, i.e.

$$C_\gamma y^2 = \psi \left[K_v N \mu p_e(y) + K_{in} N \beta S_e I_e(p_e(y)) \right], \tag{23}$$

implying

$$C_\gamma = \psi \frac{N\mu}{y^2} \left[K_v p_e(y) + K_{in}(p_c - p_e(y)) \right], \tag{24}$$

which provides a baseline estimate for C_γ.

4 Results: numerical solution of the OC problem by FBS algorithm

4.1 Numerical algorithm

In this section the optimality system given by (22), (16), (19), (20) and (21) is solved numerically by the *FBS* algorithm described in Lenhart and Workman (2007), and whose convergence is shown in Hackbusch (1978) (see also McAsey et al. 2012).

The process begins with an initial guess on the control variable. Then the state equations (22) with initial data (16) are solved with a forward in time Runge-Kutta routine. Using those new state values, the adjoint equations (19) with final data (20) are solved backward in time with the Runge-Kutta solver. The control is updated by putting the new values of states and adjoints into the characterization (21) and using a convex combination of the previous and current control estimates. The process is repeated until either convergence occurs or a maximum number of iterations has been reached. In the latter case, the computation process is marked as 'not converging'. We built a MATLAB code (Lenhart and Workman 2007; MATLAB 2015) to perform the simulations.

4.2 The structure of the OC function

As mentioned above, in our simulations we used either $\gamma_{\max} = 0.5\alpha p_c^2$ or $\gamma_{\max} = 0.7\alpha p_c^2$, thereby ruling out the possibility of disease elimination. Further, we set $\psi = 1$ and $y = \alpha p_c^2$ in formula (24) to assign a baseline value to communication costs. This gives a parsimonious baseline where the steady—state cost for the PHS communication effort is identical to the steady—state cost for vaccination in the case where infection is eliminated. Indeed, for the chosen y it is $p_e(y) = p_c$ in (6)). The OC function resulting from previous hypotheses sets at γ_{max} for the largest part of the time horizon. This can be see in right panels of Figs. 1, 2 and 3, which report the optimal control time profiles. This result follows from the disproportion between the unit cost of the policy (i.e., the sum of the unit vaccination cost and the unit communication cost) and the disease-related unit cost, which remains substantially larger. Close to the end of the horizon the control rapidly switches to zero.

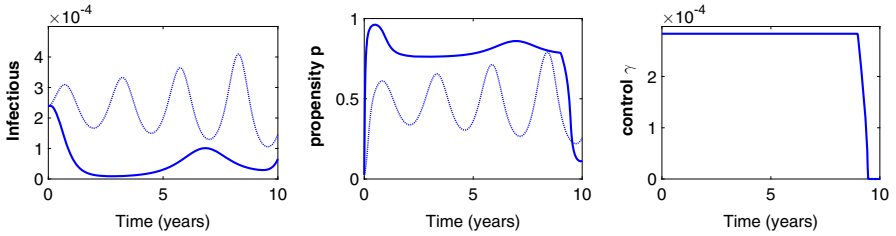

Fig. 1 Parameters of case C1 ($k = 1/10$, $\theta_1 = 2000$) and $\gamma_{\max} = 0.7\alpha p_c^2$. Left and center plots: dynamics of the system without control (system (22) with $\gamma = 0$) (dotted lines) and the controlled system (solid lines). Right plot: time profile of the optimal control. Initial data correspond to minimum value of p when the system is uncontrolled, that is: $S(0) = 0.0999972$, $I(0) = 2.3878 \times 10^{-4}$, $p(0) = 0.0256077$

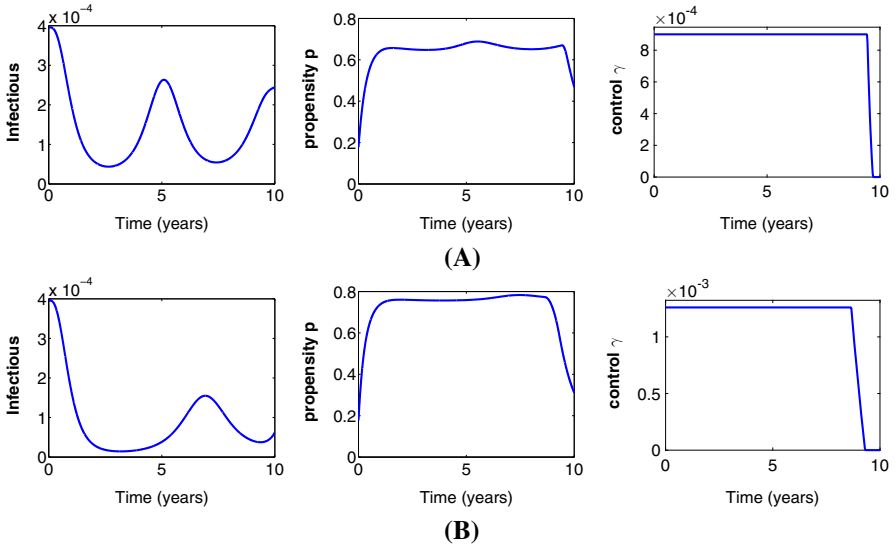

Fig. 2 Parameters of case C2 ($k = 1/90$, $\theta_1 = 450$). **a** $\gamma_{\max} = 0.5\alpha p_c^2$; **b** $\gamma_{\max} = 0.7\alpha p_c^2$. The initial data correspond to the endemic equilibrium (2) of system (1)

4.3 Role of behavioral parameters

We now focus on the interplay between key behavioral parameters (the imitation coefficient k and the relative risk of infection θ_1) and the control upper bound $\gamma_{\max}$, in affecting the system dynamics.

Figure 1 reports the solutions of the controlled system for case C1 in Sect. 3.2 ($k = 0.1$, $\theta_1 = 2000$), $\gamma_{\max} = 0.7\alpha p_c^2$. Initial data correspond to the minimum value of p for system (22) with $\gamma = 0$, i. e. $p_{\min} = 0.02561$. The corresponding initial values are $S(0) = 0.0999$, $I(0) = 2.3878 \times 10^{-4}$. This case is of interest as it represents a worst initial scenario for the public communication campaign, since the vaccine uptake is set at its minimum level (which is generally unknown to the public health planners). Figure 1 shows that despite the unfavorable initial conditions, a good result in the control of the disease is achieved, with a sharp decrease of the

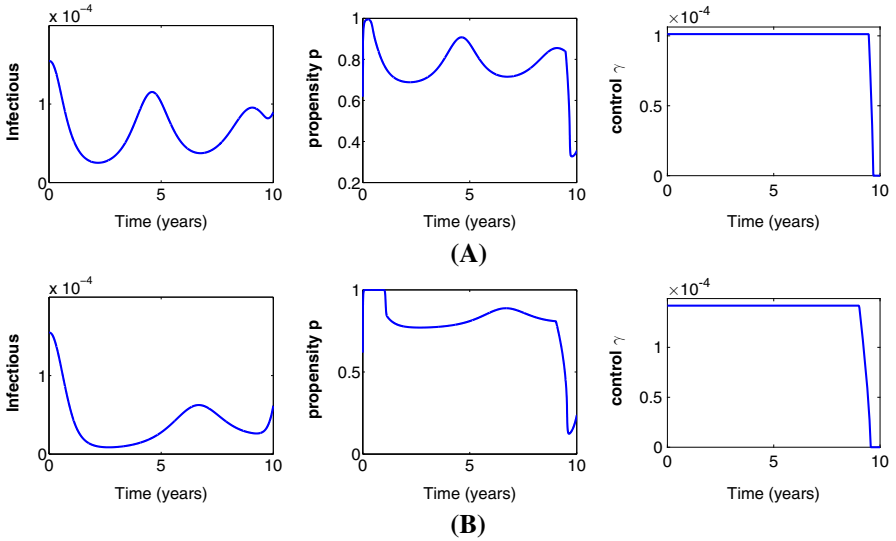

Fig. 3 Parameters of case C3 ($k = 9/10$, $\theta_1 = 4000$). **a** $\gamma_{\max} = 0.5\alpha p_c^2$; **b** $\gamma_{\max} = 0.7\alpha p_c^2$. The initial data correspond to the endemic equilibrium (2) of system (1)

infective prevalence. The next peak in prevalence (occurring seven years after the start of the communication campaign) is more than halved compared to the initial level of prevalence. Moreover, a quite high average vaccine uptake is maintained for most of the intervention horizon.

More in depth, the propensity to vaccinate in the first few months of the program moves from negligible levels to about 95%, which is above the critical vaccination threshold $p_c = 90\%$. The propensity starts declining 18 months after the initiation of the programme, setting to quite sub-optimal levels in the range of 80%. Given that $\gamma^*(t) \approx \gamma_{\max}$ for most of the horizon (Fig. 1)—which means that the perceptions about benefits and costs of immunization communicated by the PHS remain constant—it follows that the decline in coverage stems entirely from the changed perceptions of risks communicated among parents through their spontaneous contacts. This perception, indeed, is declining due to the declining prevalence. This favors the relapse of the infection bringing the new wave described above. In turn, this yields—the communication effort being still constant—a moderate relapse of p. This relapse however just lasts the duration of the epidemic wave, because the subsequent decline in the perceived risk of infection at the end of the wave brings a new phase of low perceived benefit from vaccination. The decline in the propensity to vaccinate follows the disappearance of the epidemic wave with some delay. This lag is essentially related to the magnitude of the imitation speed. Finally, as far as the impact of the control is concerned, we note that although the control $\gamma(t)$ assumes 'small' values its impact is large. First, as we noticed above, because a good decrease of the disease prevalence and a good increase of the vaccine uptake rate are predicted. Second, in the absence of control the objective functional is $27.94 * 6 * 10^7$ *USD*, whereas in the optimally

controlled scenario the cost reduces to $11.03 * 6 * 10^7$ *USD*, i.e. a reduction of 60.52% of the costs.

Figure 2 illustrates case C2 in Sect. 3.2 ($k = 1/90$, $\theta_1 = 450$). The initial data correspond to the endemic equilibrium (2) of system (1). We in particular compare the effects of different levels of the control upper bound $\gamma_{\max}$, which is set to $\gamma_{\max} = 0.5\alpha p_c^2$ (Fig. 2a), and to $\gamma_{\max} = 0.7\alpha p_c^2$ (Fig. 2b), respectively. The optimal dynamics is qualitatively similar to Fig. 1. In particular, the larger value of $\gamma_{\max}$ (Fig. 2b)) promotes a larger vaccine uptake, inducing a lower prevalence and delaying the next epidemics, compared to Fig. 2a. The pattern in the propensity to vaccinate is more regular (indeed almost constant for most of the horizon) compared to Fig. 1. This is the consequence of the very low level of the imitation speed, given the short horizon, and the lower perceived risk from infection which, jointly considered, make it negligible the impact of the evolution in the prevalence on vaccination payoff.

Finally, in Fig. 3 we consider case C3 in Sect. 3.2, assuming both a large imitation speed ($k = 0.9$) and a very large perceived risk of infection ($\theta_1 = 4000$), while still comparing the effects of different levels of the control upper bound $\gamma_{\max}$ (Fig. 3a, b). The higher perceived risk of infection, compared to Fig. 2, allows to achieve higher coverage levels, with temporary peaks as high as 100%. However, these peaks are not maintained, primarily due to the fast decline in the perceived risk of infection but also to the increased perceived risk of vaccine adverse events (caused by the large number of immunizations) whose occurrence is fastly communicated among parents thanks to the large value of the imitation speed. As in the case of Fig. 2 also here the propensity to vaccinate p achieves larger levels on average, which increases the duration of the post-vaccination *honey-moon* phase (Anderson et al. 1992) by delaying (and mitigating) the onset of the first epidemic wave (see Fig. 3b).

These scenarios are representative of the system behavior over a wide spectrum of parameter values.

5 Results: numerical solution of the OC by Simulated annealing

5.1 Simulated annealing for piecewise-constant control problems

Public health interventions such as programs to favor vaccinations by reducing parental hesitancy or refusal can be very complex and multi-layered (Sadaf et al. 2013). Thus, logistic and practical constraints make a time-continuous updating of the policy difficult. Thus, controls in a given finite time interval $[0, t_f]$ should rather be piecewise constant, of the form:

$$u(t) = \sum_{j=0}^{j_{max}} u_j Ind(t, [j\tau, (j+1)\tau)), \tag{25}$$

where the u_j are suitable constants, τ is a positive discretization step, $(j_{max}+1)\tau = t_f$ and $Ind(t, W)$ denotes the indicator function of a given set W. Note that the control horizon $[0, t_f]$ could be discretized by assuming a non constant discretization step.

We used a constant step τ for the sake of the simplicity and to mimic seasonal PH activity plans. Then, given the general n-dimensional ODE control system depending on the control $u(t)$:

$$\dot{x}(t) = F(x(t), u(t)), \tag{26}$$

let us seek the control u that minimizes the functional

$$J(u(.)) = \psi(x(t_f; u(.), x_0), u(t_f)) + \int_0^{t_f} L(x(t; u(.), x_0), u(t))dt, \tag{27}$$

under constraint

$$u_{min}(t) \leq u(t) \leq u_{max}(t), \tag{28}$$

where the control action u has the form (25) and is enacted on a time interval $[0, t_f]$.

By defining the vector $a = (u_0, \ldots, u_N)$, where $N = \left[t_f/\tau\right]$, system (26) can be rewritten as the following ODE system depending on the real vector parameter a:

$$\dot{x}(t) = f(x(t); a). \tag{29}$$

This implies that under a piecewise-constant intervention, the original OC problem transforms into the problem of nonlinear constrained optimization (NCO) of the following function of the real parameter a:

$$J(a) = \psi_1(x(t_f; a, x_0), a_N) + \int_0^{t_f} L_1(x(t; a, x_0), a)dt, \tag{30}$$

under constraint $a \in \Omega$, where (28) yields

$$\Omega = \prod_{i=1}^{N} \left[\max_{t \in T_i} u_{\min}(t), \ \min_{t \in T_i} u_{\max}(t) \right]; \quad T_i = [i\tau, (i+1)\tau].$$

This NCO problem still involves the solution of the dynamical system (29) and the application of functional operators (the integral), which will have to be numerically solved. Traditional numerical algorithms for NCO problems suffer the shortcoming that they often stuck to local minima (Henderson et al. 2003; Salamon et al. 2002). To remedy this drawback, various stochastic optimization algorithms (SOA) exploring the relevant parametric space through a random walk have been proposed (Banga and Seider 1996; Schoen 1991).

The SA is one of the most widely adopted SOA and the description is as follows (see Henderson et al. 2003; Salamon et al. 2002 for further details): the random walk in the SA algorithm is initialized from a value $a_0 \in \Omega$ which should be sufficiently close to the global minimum a^{min} (what is called an *educated guess*). Let $J(a_0)$ denote the corresponding value of the objective function. Then a random value a_1 is drawn in the neighborhood of a_0 from a suitable 'bell-shaped' or 'disk-shaped' (i.e. uniform on an hypersphere in a given norm) probability density function (PDF) ρ. If a_1 is suitable (i.e., inside Ω), then the corresponding value $J(a_1)$ is computed. Unlike deterministic

algorithms (where a_1 would be accepted if $J(a_1) \leq J(a_0)$ and rejected otherwise), in the SA algorithm if

$$J(a_{i+1}) > J(a_i),$$

then a_{i+1} can be accepted or rejected by a Boltzmann-like probabilistic rule. The rationale for this is exactly avoiding to be stuck at a local minimum.

The probabilistic rule adopted by the SA algorithm is as follows (Henderson et al. 2003; Salamon et al. 2002):

$$\exp\left(-\frac{J(a_{i+1}) - J(a_i)}{k_b T_{m(i)}}\right) < r,$$

where r is a random number uniformly distributed in (0, 1), and $T_{m(i)}$ is the 'temperature', i. e. an artificial tuning parameter which is gradually decreasing up to zero as $m(i)$ increases:

$$\lim_{i \to \infty} T_{m(i)} = 0.$$

In fact, this algorithm is inspired by Statistical Physics, where the reduction of the temperature (annealing) of a system leads it to a state of global minimal energy, here represented by the function to be minimized (Henderson et al. 2003; Salamon et al. 2002). A number of implementations of SA are available using different rules of decreasing $T_{m(i)}$ and for adjusting the PDF ρ (Faber et al. 2005; Henderson et al. 2003; Salamon et al. 2002).

5.2 Optimal PHS communication plans by SA

In this section we apply the SA approach to compare the optimal solutions with that provided by the FBS algorithm, and also to find solutions for those parametric values for which FBS failed to converge. The lack of convergence occurred for large values of the communication cost C_γ. As a further hypothesis, we assume that the communication campaigns enacted by the PHS are updated every three months, so that $\tau = 90\ days$ in (25).

We proceed as follows: first, a candidate global optimal solution is discretized at times $t_0, t_1, \ldots, t_n$ to obtain a vector l (the 'educated guess'). To this aim, when possible, the OC solution produced by the FBS algorithm is employed. Next, we set $a_0 = l$ and the SA algorithm is run.

If the optimum $u(t)$ found by the SA algorithm is far from γ^*, then it is reasonable to assume that the candidate solution is not a global minimum. In the contrary case, it would be reasonable to assume that $\gamma^*(t)$ is the real global minimum.

Since the SA algorithm is a stochastic process, it produces different outputs (in our case, the values of the vector parameter a and values of the functional J) at each run. For this reason, for each set of parameters and initial conditions, the algorithm

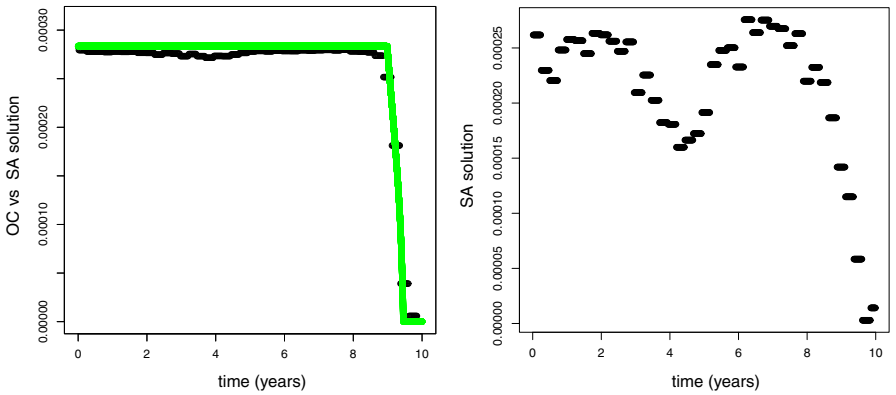

Fig. 4 SA-based search for the optimal control. Left Panel: plot of the SA optimal solution vs. the plot of the continuous OC solution. Parameters and initial values as in Fig. 1. Right panel: plot of the computed SA optimal solution. The same parameters of the left panel were adopted, but one, C_γ, which is here five times larger than the baseline case

is applied several times and then it is taken as the candidate optimal control the one corresponding to the smallest evaluated value of J.

We have performed the SA-based optimizations by using the same parameter values used in the previous section. The left panel of Fig. 4 reports both the continuous control $\gamma^*(t)$ obtained by the FBS algorithm, and the optimal piecewise constant control u obtained by the SA. It is interesting to note that although the ideal and approximate control have different nature (the former is continuous, the latter is piecewise constant), they overlap very well. As regards the values of the cost functional J, the minimum observed with the piecewise control is $J_{SA} = 11.09 \times 6 \times 10^7$, while the minimum corresponding to the continuous control is essentially identical: $J_{FBS} = 11.03 \times 6 \times 10^7$. This implies that the idealized solution is well validated by the piece-wise control.

In the other cases, there is a general agreement of the computed minima J although in the cases computed by applying SA the value is slightly larger (see Table 2).

The OC solutions obtained for the piece–wise control with the SA algorithm are similar—in our simulations—to the continuous ones obtained by using FBS algorithm. However, some appreciable local deviations and oscillations can be observed. These deviations might be due to the fact that the functional J close to its minima is quite 'flat', thus allowing to local deviations that may be quite significant.

We have also performed further simulations, which could not be performed by using the FBS algorithm due to lack of convergence in the software we used. We have assumed a larger cost coefficient for the control, namely a five-fold larger C_γ. These larger values of C_γ were employed to assess how the control changed in the case of substantially larger costs for the Public Health campaigns aimed at increasing the propensity to vaccinate. We have obtained a radically different OC solution compared with the simulations with the baseline C_γ (see right panels of Figs. 4, 5a, 6a). Indeed, in all cases the obtained control was strongly non-monotone. Of course, due to the remarkable increase of the cost associated to the control, all these OC solutions are smaller than the corresponding solutions found in the case with the baseline C_γ.

Table 2 Key features and results of the simulated scenarios

Scenario	k	θ	$\frac{\gamma_{max}}{\alpha p_c^2}$	IC	C_γ	$\frac{J_{SA}}{N}$	$\frac{J_{FBS}}{N}$	αp_c^2
Figures 1 and 4left	0.1	2000	0.7	ID_{pm}	6333	11.09	11.03	4.05×10^{-4}
Figures 1 and 4right	0.1	2000	0.7	ID_{pm}	5*6333	16.81	–	4.05×10^{-4}
Figures 2a and 5A1	1/90	450	0.5	E_{u0}	320.63	20.12	19.46	1.8×10^{-3}
Figures 2a and 5A2	1/90	450	0.5	E_{u0}	5*320.63	24.43	–	1.8×10^{-3}
Figures 2b and 5B1	1/90	450	0.7	E_{u0}	320.63	14.65	14.45	1.8×10^{-3}
Figures 2b and 5B2	1/90	450	0.7	E_{u0}	5*320.63	20.43	–	1.8×10^{-3}
Figures 3a and 6A1	0.9	4000	0.5	E_{u0}	25330	11.83	11.67	2.02×10^{-4}
Figures 3a and 6A2	0.9	4000	0.5	E_{u0}	5*25330	14.54	–	2.02×10^{-4}
Figures 3b and 6B1	0.9	4000	0.7	E_{u0}	25330	9.52	9.40	2.02×10^{-4}
Figures 3b and 6B2	0.9	4000	0.7	E_{u0}	5*25330	14.55	–	2.02×10^{-4}

ID_{pm} indicates initial data corresponding to minimum value of p when the system is uncontrolled. E_{u0} indicates that the initial data correspond to the endemic equilibrium (2) of system (1)

Finally, with regards to the obtained numerical values for J, in all cases they are larger than the baseline corresponding cases, as reported in Table 2.

6 Concluding remarks

Under voluntary vaccination for childhood diseases, modeling of immunization campaigns is quite complex since coverage is the outcome of parents' decisions. However, the PHS can enact actions aimed at contrasting policy-resistant behaviors by enforcing its role as the most influential provider of information about the infection and vaccines, and related benefits and costs. Our work is aimed at determining the optimal control of the effort of PHS in the framework of Behavioral Epidemiology.

We found that under many circumstances the resulting OC time-profile rapidly sets at its maximum admissible value, where it remains for the largest part of the time horizon. This result follows from the disproportion between the unit cost of the policy (i.e., the sum of the unit vaccination cost and the unit communication cost) and the costs induced by the disease. Indeed, for childhood diseases the latter cost is substantially larger than the former ones. The setting of the control effort at its maximum level means that the perceptions about the net benefit of immunization communicated by the PHS cannot be increased any further. This suggests that the subsequent dynamics stems entirely from the changed perceptions of risks (i.e., mostly the declining perceived risk of infection due to the declining prevalence) communicated among parents through spontaneous contacts. This leads, sooner or later, to a future decline in vaccine uptake triggered by the success in controlling infection during the first phase of the program. Although, in the case of baseline C_γ from mathematical point of view there is not so much difference between the cost associated to a constant control with respect to the cost associated to the OC solution we found, from the practical Public Health

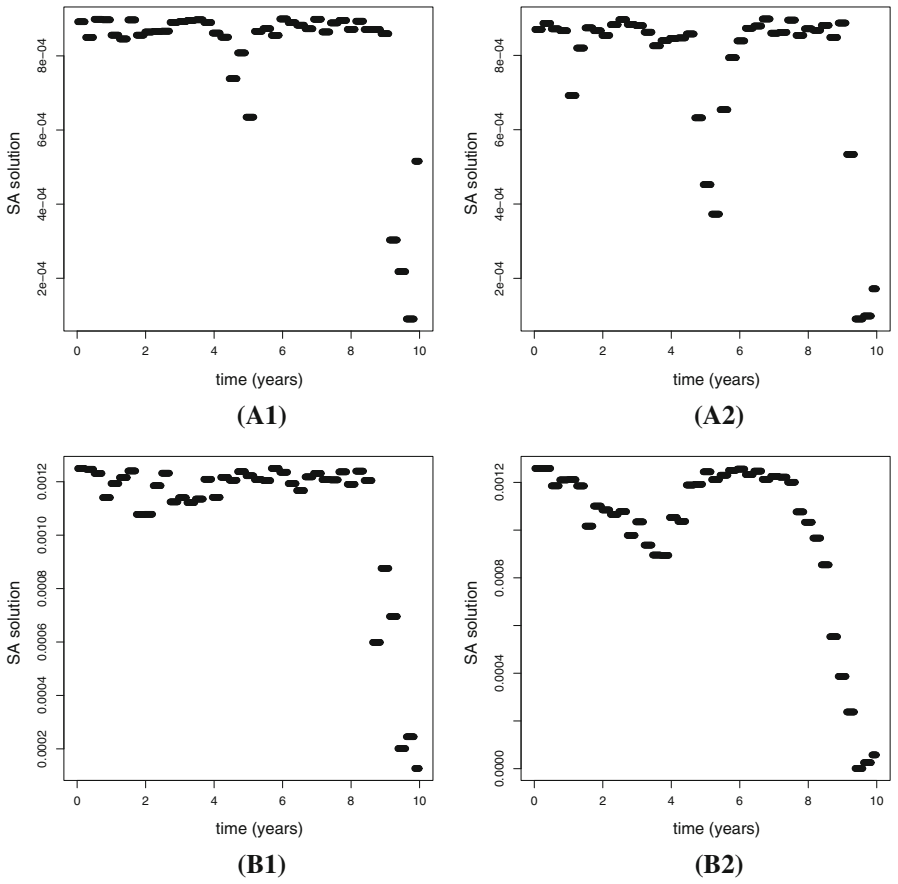

Fig. 5 Plots of the computed SA optimal solutions. Parameters of case C2 ($k = 1/90$, $\theta_1 = 450$). **a** $\gamma_{\max} = 0.5\alpha p_c^2$. **b** $\gamma_{\max} = 0.7\alpha p_c^2$. (A1) and (B1) C_γ as in Fig. 2. (A2) and (b2) C_γ five times larger

viewpoint a difference exists. Indeed, using a constant control even for all the time horizon (i.e. even when our OC solution is zero) implies that one has to maintain a considerable amount of activities (some of which at no cost, e.g. voluntary efforts by GPs), moreover at a cost that is greater than in absence of any work.

We feel that this results might contribute to clarify some of the difficulties met by PHS systems in maintaining high coverages for common vaccine preventable infections.

For large PHS action-related costs, we obtained that the OC is non-monotone, in some cases exhibiting oscillations. Unfortunately, in case of larger C_γ the FBS algorithm did not converge, so that we could not assess, in the continuous case, the effects of the upper limit constraints γ_{max}. However, this is fully done with the SA algorithm.

As far as the control modeling is concerned, we stressed the relevance of modeling the effort by the PHS as a piecewise constant function. This called for the use of the SA optimization algorithm.

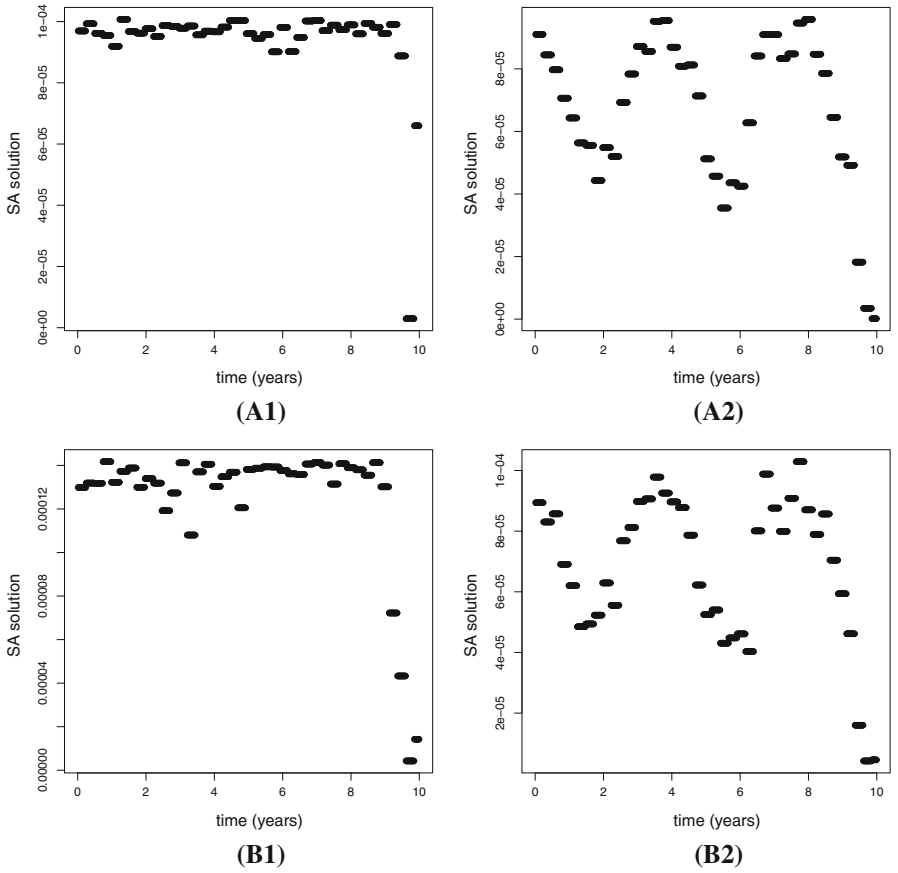

Fig. 6 Plots of the median of the computed 101 SA optimal solutions. Parameters of case C3 ($k = 9/10$, $\theta_1 = 4000$). **a** $\gamma_{\max} = 0.5\alpha p_c^2$. **b** $\gamma_{\max} = 0.7\alpha p_c^2$. (A1) and (B1) C_γ as in Fig. 3. (A2) and (B2) C_γ five times larger

Our results show that the OC solutions obtained by using the FBS and those obtained by the SA algorithms stay overall close. By employing SA algorithm large local deviations and local stochastic fluctuations are observed, which suggests that the minimum corresponding to the OC solution for the considered problem might be quite 'flat'. Therefore, in our problem, even alternative controls that have local remarkable deviations are very close to the global minimum. In this sense, the classical OC solution seems to be relatively robust with respect to deviations imposed by the practical implementation of the communication program.

As far as the modeling of intervention costs are concerned, we provided an example where a quadratic cost—often adopted as a proxy of more complex nonlinear costs—can be justified based on simple PH reasoning. On the other hand, the behavioural epidemiology investigations on public vaccine awareness is very recent and mostly relying on qualitative results (Consortium; IMI 2018) so that quantitative studies based on appropriate data are yet to come.

As regards the adopted model of disease spread, the first and strongest limitation of our work is that we employed a simple SIR deterministic model (complemented by an imitation equation for the vaccination propensity) without age structure. Though, from an historical viewpoint, the simple deterministic SIR model was able to provide important qualitative hints to Public Health authorities (Anderson et al. 1992) as well as a robust base upon which to build more realistic models, it is nowadays well known that this model is not able to provide adequate quantitative predictions on the spread and control of an infectious disease in the real world. Thus the present study has to be intended as a crude first order approximation of a real scenario. A slightly better (although still insufficient) approximation would require the inclusion of internal (Andersson and Britton 2012) and external (Øksendal 2003) randomness. They would require the application of methodologies of stochastic optimal control for, respectively, birth and death epidemic processes (Lefévre 1981; Getz 1975) and for stochastic differential systems (Fleming and Rishel 2012, 1975). In turn, both deterministic and stochastic SIR model with and without age structure suffer of a common important limitation: they focus on the spread and control of a single isolated target population. This is seldom the case in the real world, so that a stochastic meta-population approach (Keeling and Rohani 2011; Ajelli et al. 2010) including age structured social (Melegaro et al. 2017) contacts would ultimately be necessary to provide more realistic suggestions to Public Health authorities.

As far as the actual model of the PHS intervention is concerned, we stress that here we adopted a practical viewpoint where we defined as effort the control $\gamma(t)$, which more realistically should instead be considered as the 'impact of the effort'. A function or even better a dynamical system connecting the real effort $E(t)$ and $\gamma(t)$ should, thus, complete the dynamical system in study. Note, however, that the exact definition and properties of the relationship between $E(t)$ and $\gamma(t)$ are both nontrivial. Another important point is the investigation of more realistic functional forms to sdescribe the per-capita costs for the PHS to realize strategy switching, i.e. the functional $A(\gamma(t), a(t))$.

Summarizing, the present work is only a first and quite elementary step towards the definition of a far more complete model of the impact of PHS efforts to spread the awareness of the importance of vaccines and, as a consequence, to increase vaccine uptake.

Acknowledgements The work of B. B. has been performed under the auspices of the Italian National Group for the Mathematical Physics (GNFM) of National Institute for Advanced Mathematics (INdAM). We wish to acknowledge the two anonymous referees, whose suggestions helped us to significantly increase the quality and the readability of this work.

References

Ajelli M, Gonçalves B, Balcan D, Colizza V, Hu H, Ramasco JJ, Merler S, Vespignani A (2010) Comparing large-scale computational approaches to epidemic modeling: agent-based versus structured metapopulation models. BMC Infect Dis 10(1):190

Anderson RM, May RM, Anderson B (1992) Infectious diseases of humans: dynamics and control, vol 28. Wiley Online Library, New York

Andersson H, Britton T (2012) Stochastic epidemic models and their statistical analysis. Springer, New York
Aniţa S, Capasso V, Arnăutu V (2011) An introduction to optimal control problems in life sciences and economics. Birkhäuser/Springer, New York
Asano E, Gross LJ, Lenhart S, Real LA (2008) Optimal control of vaccine distribution in a rabies metapopulation model. Math Biosci Eng 5(2):219–238
Banga JR, Seider WD (1996) Global optimization of chemical processes using stochastic algorithms. In: Floudas C, Pardalos PM (eds) State of the art in global optimization. Springer, New York, pp 563–583
Bauch CT (2005) Imitation dynamics predict vaccinating behaviour. Proc R Soc Lond B Biol Sci 272(1573):1669–1675
Betta M, Laurino M, Pugliese A, Guzzetta G, Landi A, Manfredi P (2016) Perspectives on optimal control of varicella and herpes zoster by mass routine varicella vaccination. Proc R Soc B 283(1826):20160054
Blayneh KW, Gumel AB, Lenhart S, Clayton T (2010) Backward bifurcation and optimal control in transmission dynamics of west nile virus. Bull Math Biol 72(4):1006–1028
Bolzoni L, Tessoni V, Groppi M, De Leo GA (2014) React or wait: which optimal culling strategy to control infectious diseases in wildlife. J Math Biol 69(4):1001–1025
Buonomo B (2011) A simple analysis of vaccination strategies for rubella. Math Biosci Eng 8:677–687
Buonomo B, dOnofrio A, Lacitignola D (2013) Modeling of pseudo-rational exemption to vaccination for seir diseases. J Math Anal Appl 404(2):385–398
Buonomo B, Carbone G, d'Onofrio A (2018) Effect of seasonality on the dynamics of an imitation-based vaccination model with public health intervention. Math Biosci Eng 15(1):299–321
Capasso V (1993) Mathematical structures of epidemic systems. Springer, Berlin
Carabin H, Edmunds WJ, Kou U, Van den Hof S, Van Hung N (2002) The average cost of measles cases and adverse events following vaccination in industrialised countries. BMC Public Health 2(1):22
Chamchod F, Cantrell RS, Cosner C, Hassan AN, Beier JC, Ruan S (2014) A modeling approach to investigate epizootic outbreaks and enzootic maintenance of rift valley fever virus. Bull Math Biol 76(8):2052–2072
Choi S, Jung E (2014) Optimal tuberculosis prevention and control strategy from a mathematical model based on real data. Bull Math Biol 76(7):1566–1589
Demasse RD, Tewa J-J, Bowong S, Emvudu Y (2016) Optimal control for an age-structured model for the transmission of hepatitis B. J Math Biol 73(2):305–333
d'Onofrio A, Manfredi P, Salinelli E (2007) Vaccinating behaviour, information, and the dynamics of sir vaccine preventable diseases. Theor Popul Biol 71(3):301–317
d'Onofrio A, Manfredi P, Poletti P (2011) The impact of vaccine side effects on the natural history of immunization programmes: an imitation-game approach. J Theor Biol 273(1):63–71
d'Onofrio A, Manfredi P, Poletti P (2012) The interplay of public intervention and private choices in determining the outcome of vaccination programmes. PLoS ONE 7(10):e45653
Doutor P, Rodrigues P, Soares MC, Chalub FACC (2016) Optimal vaccination strategies and rational behaviour in seasonal epidemics. J Math Biol 73(6–7):1437–1465
Faber R, Jockenhövel T, Tsatsaronis G (2005) Dynamic optimization with simulated annealing. Comput Chem Eng 29(2):273–290
Fister KR, Lenhart S, McNally JS (1998) Optimizing chemotherapy in an hiv model. Electron J Differ Equ 1998(32):1–12
Fleming WH, Rishel RW (1975) Deterministic and stochastic optimal control, vol 1 of applications of mathematics. Springer, Berlin
Fleming WH, Rishel RW (2012) Deterministic and stochastic optimal control. Springer Science & Business Media, New York
Funk S, Salathé M, Jansen VAA (2010) Modelling the influence of human behaviour on the spread of infectious diseases: a review. J R Soc Interface 7:1247–1256
Gaff H, Schaefer E (2009) Optimal control applied to vaccination and treatment strategies for various epidemiological models. Math Biosci Eng MBE 6(3):469–492
Getz WM (1975) Optimal control of a birth-and-death process population model. Math Biosci 23(1–2):87–111
Hackbusch W (1978) A numerical method for solving parabolic equations with opposite orientations. Computing 20(3):229–240
Hansen E, Day T (2011) Optimal control of epidemics with limited resources. J Math Biol 62(3):423–451

Henderson D, Jacobson SH, Johnson AW (2003) The theory and practice of simulated annealing. In: Gendreau M, Potvin JY (eds) Handbook of metaheuristics. Springer, Boston, pp 287–319
Hethcote HW, Waltman P (1973) Optimal vaccination schedules in a deterministic epidemic model. Math Biosci 18(3–4):365–381
Hofbauer J, Sigmund K (1998) Evolutionary games and population dynamics. Cambridge University Press, Cambridge
IMI (2018) Innovative medicine initiative. First innovative medicines initiative ebola projects get underway. www.imi.europa.eu/content/ebola-project-launch. Accessed January 2018
Joshi HR (2002) Optimal control of an HIV immunology model. Optim Control Appl Methods 23(4):199–213
Jung E, Lenhart S, Feng Z (2002) Optimal control of treatments in a two-strain tuberculosis model. Discrete Continuous Dyn Syst Ser B 2(4):473–482
Jung E, Iwami S, Takeuchi Y, Jo T-C (2009) Optimal control strategy for prevention of avian influenza pandemic. J Theor Biol 260(2):220–229
Kassa SM, Ouhinou A (2015) The impact of self-protective measures in the optimal interventions for controlling infectious diseases of human population. J Math Biol 70(1–2):213–236
Keeling MJ, Rohani P (2011) Modeling infectious diseases in humans and animals. Princeton University Press, Princeton
Kirkpatrick S, Gelatt CD, Vecchi MP (1983) Optimization by simulated annealing. Science 220(4598):671–680
Laguzet L, Turinici G (2015a) Global optimal vaccination in the sir model: properties of the value function and application to cost-effectiveness analysis. Math Biosci 263:180–197
Laguzet L, Turinici G (2015b) Individual vaccination as nash equilibrium in a sir model with application to the 2009–2010 influenza a (H1N1) epidemic in france. Bull Math Biol 77(10):1955–1984
Larson HJ, Jarrett C, Eckersberger E, Smith DM, Paterson P (2014) Understanding vaccine hesitancy around vaccines and vaccination from a global perspective: a systematic review of published literature, 2007–2012. Vaccine 32(19):2150–2159
Lee S, Castillo-Chavez C (2015) The role of residence times in two-patch dengue transmission dynamics and optimal strategies. J Theor Biol 374:152–164
Lee S, Morales R, Castillo-Chavez C (2011) A note on the use of influenza vaccination strategies when supply is limited. Math Biosci Eng 8(1):171–182
Lee S, Golinski M, Chowell G (2012) Modeling optimal age-specific vaccination strategies against pandemic influenza. Bull Math Biol 74(4):958–980
Lefévre C (1981) Optimal control of a birth and death epidemic process. Oper Res 29(5):971–982
Lenhart S, Workman JT (2007) Optimal control applied to biological models. CRC Press, London
Mahajan V, Peterson RA (1985) Models for innovation diffusion. Sage Publications Inc, Thousand Oaks
Manfredi P, d'Onofrio A (2013) Modeling the Interplay between human behavior and the spread of infectious diseases. Springer, New York
Martínez-Alfaro H (2010) Using simulated annealing algorithm to solve the optimal control problem. In Chibante R (ed) Simulated annealing, theory with applications. InTech
MATLAB (2015) Matlab release 2015a. the mathworks inc. natich, ma
McAsey M, Mou L, Han W (2012) Convergence of the forward–backward sweep method in optimal control. Comput Optim Appl 53(1):207–226
Melegaro A, Del Fava E, Poletti P, Merler S, Nyamukapa C, Williams J, Gregson S, Manfredi P (2017) Social contact structures and time use patterns in the manicaland province of Zimbabwe. PloS ONE 12(1):e0170459
Morton R, Wickwire KH (1974) On the optimal control of a deterministic epidemic. Adv Appl Probab 6(4):622–635
Neilan RLM, Schaefer E, Gaff H, Fister KR, Lenhart S (2010) Modeling optimal intervention strategies for cholera. Bull Math Biol 72(8):2004–2018
Øksendal B (2003) Stochastic differential equations. Springer, Berlin
Onyango NO, Müller J (2014) Determination of optimal vaccination strategies using an orbital stability threshold from periodically driven systems. J Math Biol 68(3):763–784
Oraby T, Thampi V, Bauch CT (2014) The influence of social norms on the dynamics of vaccinating behaviour for paediatric infectious diseases. Proc R Soc B 281:20133172
Panetta JC, Fister KR (2000) Optimal control applied to cell-cycle-specific cancer chemotherapy. SIAM J Appl Math 60(3):1059–1072

Panetta JC, Fister KR (2003) Optimal control applied to competing chemotherapeutic cell-kill strategies. SIAM J Appl Math 63(6):1954–1971
Pontryagin LS, Boltyanskii VG, Gamkrelidze RV, Mishenko EF (1962) The mathematical theory of optimal processes. (Translated from the russian by Trigoroff, K. N.). Wiley Interscience, New York
Prosper O, Saucedo O, Thompson D, Torres-Garcia G, Wang X, Castillo-Chavez C (2011) Modeling control strategies for concurrent epidemics of seasonal and pandemic H1N1 influenza. Math Biosci Eng 8(1):141–170
Rachah A, Torres DFM (2016) Dynamics and optimal control of ebola transmission. Math Comput Sci 10(3):331–342
Rodrigues P, Silva CJ, Torres DFM (2014) Cost-effectiveness analysis of optimal control measures for tuberculosis. Bull Math Biol 76(10):2627–2645
Rowthorn R, Walther S (2017) The optimal treatment of an infectious disease with two strains. J Math Biol 74(7):1753–1791
Sadaf A, Richards JL, Glanz J, Salmon DA, Omer SB (2013) A systematic review of interventions for reducing parental vaccine refusal and vaccine hesitancy. Vaccine 31(40):4293–4304
Salamon P, Sibani P, Frost R (2002) Facts, conjectures, and improvements for simulated annealing. SIAM, Philadelphia
Schättler H, Ledzewicz U (2012) Geometric optimal control: theory, methods and examples, vol 38. Springer Science & Business Media, New York
Schoen F (1991) Stochastic techniques for global optimization: a survey of recent advances. J Glob Optim 1(3):207–228
Sethi SP, Staats PW (1978) Optimal control of some simple deterministic epidemic models. J Oper Res Soc 29(2):129–136
The ASSET Consortium. Asset. eu action plan on science in society related issues in epidemics and total pandemics. www.asset-scienceinsociety.eu. Accessed January 2018
Wang Z, Bauch CT, Bhattacharyya S, d'Onofrio A, Manfredi P, Perc M, Perra N, Salathé M, Zhao D (2016) Statistical physics of vaccination. Phys Rep 664:1–113
Wickwire K (1977) Mathematical models for the control of pests and infectious diseases: a survey. Theor Popul Biol 11(2):182–238
Williamson S (2007) The vaccination controversy: the rise, reign, and fall of compulsory vaccination for smallpox. Liverpool University Press, Liverpool
Zhao S, Kuang Y, Chih-Hang W, Ben-Arieh D, Ramalho-Ortigao M, Bi K (2016) Zoonotic visceral leishmaniasis transmission: modeling, backward bifurcation, and optimal control. J Math Biol 73(6–7):1525–1560